MR-Guided Catheter Navigation of the Intracranial Subarachnoid Space

George Rappard, Gregory J. Metzger, James L. Fleckenstein, Evelyn E. Babcock, Paul T. Weatherall, Robert E. Replogle, G. Lee Pride, Jr, Susan L. Miller, Christina E. Adams and Phillip D. Purdy

AJNR Am J Neuroradiol 2003, 24 (4) 626-629
http://www.ajnr.org/content/24/4/626

AJNR Am J Neuroradiol 24:626–629, April 2003

Technical Note

MR-Guided Catheter Navigation of the Intracranial Subarachnoid Space

George Rappard, Gregory J. Metzger, James L. Fleckenstein, Evelyn E. Babcock, Paul T. Weatherall, Robert E. Replogle, G. Lee Pride Jr, Susan L. Miller, Christina E. Adams, and Phillip D. Purdy

Summary: Percutaneous intraspinal navigation (PIN) is a new minimally invasive approach to the CNS. The authors studied the utility of MR-guided intracranial navigation following access to the subarachnoid compartment via PIN. The passive tracking technique was employed to visualize devices during intracranial navigation. Under steady-state free precession (SSFP) MR-guidance a microcatheter-microguidewire was successfully navigated to multiple brain foci in two cadavers. SSFP MR fluoroscopy possesses adequate contrast and temporal resolution to allow MR-guided intracranial navigation.

Percutaneous intraspinal navigation (PIN) is a recently reported technique for navigating devices within the subarachnoid space. With the use of PIN and x-ray fluoroscopic guidance, catheters have been successfully navigated to the third and fourth ventricles, anterior and middle fossae, convexities, and sylvian fissures (1). Intrathecal microcatheters are already used in the setting of subarachnoid hemorrhage lavage (2). Steady-state free precession (SSFP) MR fluoroscopy is an available means for monitoring the navigation of catheters in the subarachnoid space, providing adequate contrast and temporal resolution to facilitate real-time MR-guided intracranial navigation.

Technique

Cadaver Study

Two unfixed cadavers were obtained through an institutional willed-bodies program. PIN was performed under x-ray fluoroscopic guidance. The cadavers were placed in the prone position, and the spinal subarachnoid space was accessed at L2–3 in case 1 and at L2–3 and L3–4 in case 2. With the use of a micropuncture set, a 6F sheath was placed over a wire into the lumbar cistern. A low-pressure sodium chloride flush was administered through the sheath to maintain distention of the subarachnoid space. A 0.035-inch glidewire (Terumo Medical Corporation, Somerset, NJ) was advanced through the sheath and navigated cranially to the foramen magnum. A 5F guide catheter (Medi-Tech, Boston Scientific, Watertown, MA) was then advanced over the wire to the foramen magnum. In case 1, the guide catheter was positioned in the ventral spinal subarachnoid space. In case 2, a guide catheter was positioned in the ventral subarachnoid space, and a second guide catheter was positioned in the dorsal spinal subarachnoid space. In both cases, 3F nitinol braided microcatheters and 0.014-inch nitinol microguidewires (Target Therapeutics, Boston Scientific, Fremont, CA) were advanced through the guide catheters and positioned at the foramen magnum. The subjects were then transported to the MR suite for MR-guided intracranial navigation.

An in-room monitor suspended from the ceiling was used during intracranial navigation. This monitor reproduced the monitor display in the control room, allowing for bedside alterations in the sequence parameters and imaging plane. MR-guided catheter navigation was carried out by GR and PDP. Device visualization was done via the passive tracking technique.

Sequence Optimization

Imaging was performed by using a 1.50-T system with 30-mT/m gradient coils (Intera; Philips Medical Systems, Best, The Netherlands). Optimization of an MR fluoroscopic sequence for brain imaging was undertaken by using human volunteers. Preliminary experiments compared the following: T2-weighted fast spin-echo (FSE) imaging, half-Fourier acquisition single-shot turbo spin-echo (HASTE) imaging, diffusion-weighted (DW) imaging, fast low-angle shot (FLASH) imaging, and balanced fast field-echo (BFFE; Philips' proprietary version of SSFP) imaging. Factors considered in selecting a sequence were the CSF-to-brain contrast, the device-to-CSF contrast, the temporal resolution, and the magnetic susceptibility artifacts at the skull base. In considering these factors, SSFP imaging was selected. In human volunteers and phantoms, the SSFP sequence was optimized for CSF-to-brain contrast, device-to-CSF contrast, and spatial temporal resolution. The SSFP sequence was optimized as follows: TR/TE/, 5.2/2.5; acquisition, 1; flip angle, 90°; matrix, 192 × 256; 75% image; section thickness, 5 mm; and FOV, 23 cm with a reduced FOV of 75%. With these parameters, an image was obtained every 552 milliseconds. A quadrature head coil was also used for imaging.

Results

Experiments with human volunteers revealed that SSFP imaging provided high CSF-to-brain contrast at ultra-fast imaging speeds. Preliminary experiments showed that images of adequate quality can be obtained in 250 milliseconds (Fig 1). SSFP

Received June 16, 2002; accepted after revision October 20.

From the Department of Radiology, Division of Neuroradiology (G.R., J.L.F., R.E.R., G.L.P., P.D.P), Department of Radiology (P.T.W.), Division of Medical Physics (E.E.B.), Department of Neurological Surgery (R.E.R., P.D.P.) and the Mobility Foundation Center (S.L.M., C.E.A., P.D.P.), the University of Texas Southwestern Medical Center at Dallas; and Philips Medical Systems (G.J.M.), Best, the Netherlands.

Presented in part at the 40th Annual Meeting of the American Society of Neuroradiology, Vancouver, British Columbia, Canada, May, 2002.

Address reprint requests to George Rappard, MD, University of Texas Southwestern Medical Center, 5323 Harry Hines Blvd, Dallas, TX 75390-8896.

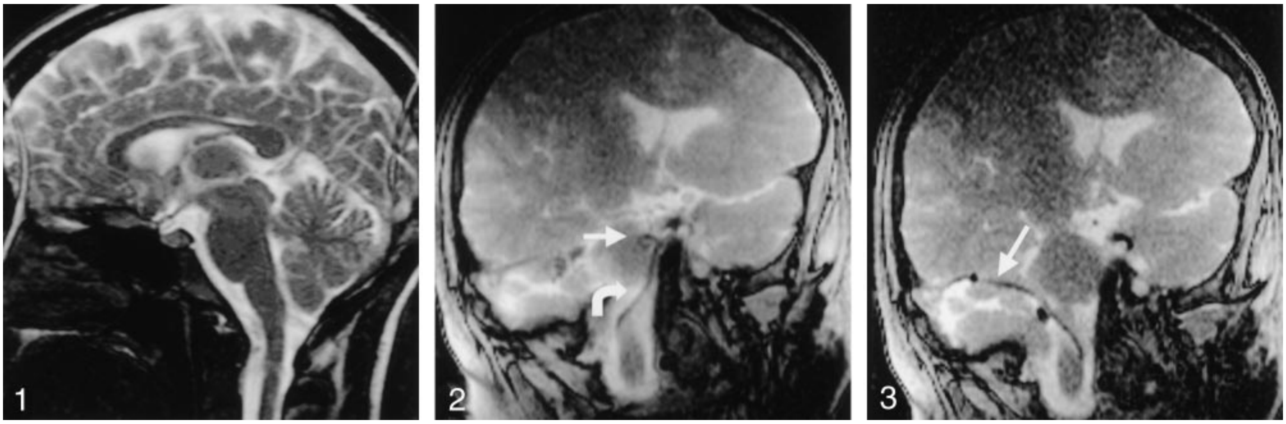

FIG 1. SSFP image in human volunteer. The image was produced in 253 milliseconds (four frames per second), with the following parameters: TR/TE, 4.4/2.2/90; flip angle, 192 × 256; section thickness, 10 mm; FOV, 200 mm; 80% reduced FOV; 60% image; and 50% keyhole. Note the paucity of CSF pulsation artifact or magnetic susceptibility effects at the skull base.

FIG 2. A 3F catheter (*curved arrow*) and 0.014-inch guidewire (*straight arrow*) are in the pontine cistern. Note that magnetic susceptibility artifact allows adequate visualization of the microguidewire.

FIG 3. The 3F microcatheter (*arrow*) traverses cerebellopontine angle.

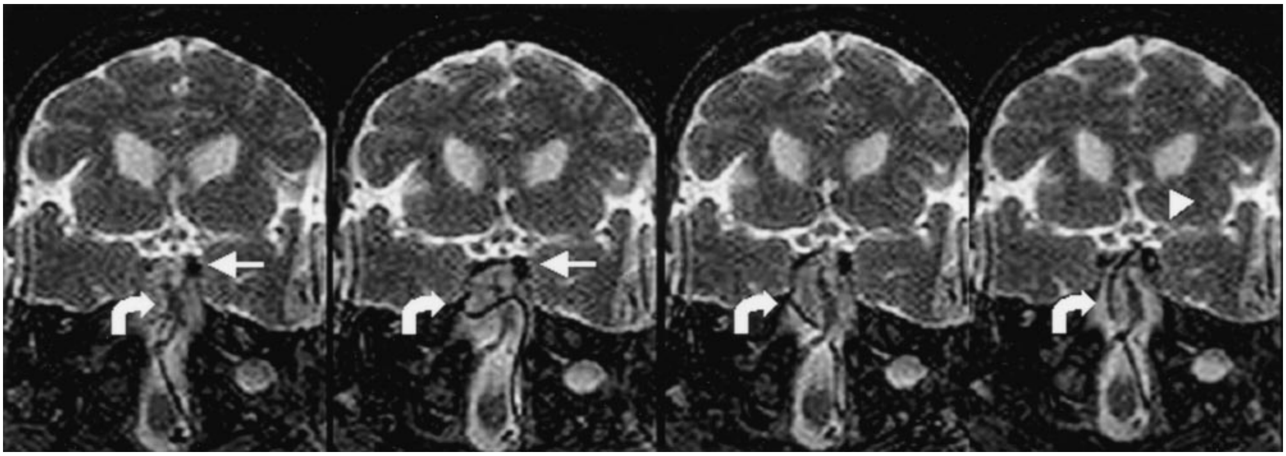

FIG 4. The catheter-guidewire (*curved arrows*) is advanced through prepontine cistern; it impacts the posterior clinoid process (*straight arrows*) and buckles in the pontine cistern. The catheter-guidewire is then redirected to suprasellar cistern and advanced to the left sylvian fissure (*arrowhead*).

fluoroscopy was resilient to degrading artifacts. CSF pulsation artifacts and skull-base susceptibility effects were negligible.

Adequate device-to-CSF contrast was present to visualize catheters and guidewires in the intracranial subarachnoid space. Device-induced magnetic susceptibility effects enhanced the visualization of a 0.014-inch nitinol microguidewire (Fig 2) without degrading artifacts. Temporal resolution was sufficient to permit continuous device visualization during MR-guided navigation. Additionally, CSF-to-brain contrast allowed adequate anatomic localization of intracranial devices. In case 1, the medullary and pontine cisterns were successfully navigated by using a ventral intraspinal approach to arrive at the cerebellopontine angle (Fig 3). In case 2, the microcatheter-microguidewire was navigated through the prepontine cistern and into the basal cisterns by using a ventral intraspinal approach. With advancement of the microcatheter-microguidewire, the catheter was noted to impact the left posterior clinoid process and was withdrawn to remove the tension, the catheter was redirected into the suprasellar cistern, and the microcatheter-microguidewire was advanced into the deep left sylvian fissure (Fig 4). In case 2, access to the cisterna magna was allowed via the dorsal intraspinal approach.

Discussion

The passive tracking system was employed to visualize devices in the MR environment. With the passive tracking technique, devices that are composed of inert, highly organized materials resistant to radiofrequency stimulation are visualized on the basis of their lack of signal. Magnetic susceptibility artifacts that are induced by the susceptibility differences between paramagnetic devices and diamagnetic tissues further enhance device visualization. These magnetic susceptibility differences result in local inhomogene-

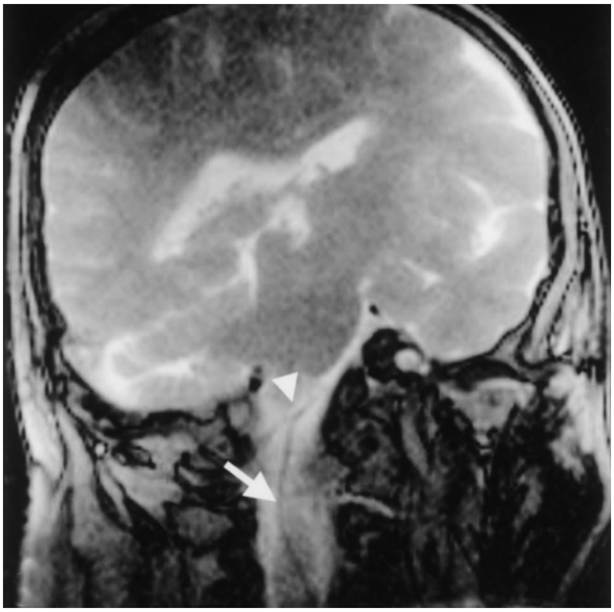

FIG 5. A 5F catheter (*arrow*) contacts the vertebral artery (*arrowhead*).

ity in the magnetic field, which affects the relaxation properties of nearby protons. The effect results in intravoxel dephasing that leads to an artifactual signal void. Importantly, devices must remain within the prescribed imaging plane in order to be visualized. In addition, device visualization is aided by the presence of intermediate or high-signal-intensity adjacent tissue and is thus sequence dependent.

In 1986 (3), Mueller et al introduced the concept of using MR imaging for intraprocedural device guidance, describing a novel method of MR imaging–guided aspiration biopsy. These authors used a spin-echo pulse sequence with a TR/TE of 50/30 to guide needle aspiration of liver metastases. Subsequently, FLASH imaging was applied to hepatic needle biopsy, offering potential acquisition speeds of less than 1 second (4). Tissue contrast, however, was dependent on time-consuming prepulses. Several authors have subsequently reported the use of SSFP MR fluoroscopically guided procedures in conjunction with the passive tracking technique. Lewin et al (5) reported their experience with percutaneous biopsy and interstitial thermal ablation of abdominal tumors. Wacker et al (6) studied the feasibility of aortic navigation in a pig. The authors were able to select the renal and splenic arteries by using the passive tracking technique. Spuentrup et al (7) reported the successful deployment of 10 of 11 stents in coronary arteries of seven pigs. The coronary catheterizations were performed during free breathing and without cardiac triggering.

SSFP imaging was first described in 1986 as fast imaging with steady-state precession (FISP) (8). The original sequence was modified to overcome artifactual banding across the FOV, at the cost of contrast and temporal resolution. With improved shimming, banding artifact was reduced, and interest in the original SSFP sequence, eg, true FISP, reemerged (9, 10). Today, SSFP sequences are known by a variety of acronyms: true FISP, fast imaging employing steady-state acquisition (FIESTA) and BFFE. In SSFP imaging, a steady state is reached when each subsequent radio-frequency pulse contributes to both longitudinal and transverse magnetization. Therefore, contrast on SSFP images is based on T2/T1 (11). T2/T1 is high for CSF and enhances its signal intensity. T2/T1 for brain is substantially lower and allows for enhanced CSF-to-brain contrast, which is "T2-like." The CSF-to-tissue contrast of SSFP imaging is recognized to have potential in CNS imaging (12). Compared with HASTE, SSFP provides improved image quality in the prenatal evaluation of the fetal brain (13). Fast imaging speeds and relatively high contrast-to-noise ratios and signal-to-noise ratios (SNRs) have made SSFP imaging useful in MR fluoroscopy. Cardiac MR fluoroscopy applications using SSFP imaging have shown that it provides improved image quality compared with FSE and FLASH imaging (13, 14).

SSFP MR fluoroscopy can provide tissue contrast and temporal resolution suitable for the selection of discreet intracranial foci after the subarachnoid compartment is entered by means of PIN. In case 1, the medullary and pontine cisterns were successfully navigated by using a ventral intraspinal approach to arrive at the cerebellopontine angle (Fig. 3).

The image quality achieved with SSFP MR fluoroscopy may be beneficial in monitoring the relationship between the devices and the adjacent structures. This information then might be used to redirect those devices away from critical brain structures. Navigating in the pontomedullary cistern in case 1, contact was made between the guide catheter and the vertebral artery (Fig 5). The device was withdrawn and remanipulated to avoid contact with vascular structures. The contrast in SSFP MR fluoroscopy can also be exploited to avoid brain penetration. This contrast is enhanced by the use of smaller flip angles, which increase the device-to-brain contrast when the passive tracking technique is used. The ability to visualize cerebral structures while maintaining the temporal resolution needed to navigate the devices intracranially is a notable advantage of this method compared with x-ray fluoroscopy.

A notable advantage of accessing the intracranial compartment with PIN is that this approach allows the use of a conventional configuration 1.5-T or one with a higher field strength magnet for imaging. The operator stands at the level of the subject's lumbar cistern and advances the microcatheter-microguidewire cranially, toward the isocenter of the magnet. The use of a closed-bore, high-field-strength magnet results in an improved SNR and temporal resolution compared with that of an open configuration magnet. The relative advantage of using a 1.5-T or higher system would thus be apparent during device manipulation.

The artifacts seen with SSFP fluoroscopy were minor. In human volunteers, CSF pulsation artifacts and skull-base susceptibility effects were negligible. Device-induced magnetic susceptibility effects permitted the visualization of a 0.014-inch nitinol microguidewire (Fig 2) without substantial degrading artifacts. Magnetic susceptibility artifacts tend to be greater with the use of gradient-echo–based sequences, such as SSFP, and the use of high-strength external magnetic fields. Both of these factors were considerations in this experiment. The use of nitinol, a nickel-titanium nonferromagnetic alloy, in the microcatheter braiding and microguidewire allowed for sufficient artifact to enhance device visibility without reducing image quality.

Although MR fluoroscopic frame rates of approximately 20 frames per second are possible on modern machines, such frame rates are excessive, and the corresponding images often lack adequate contrast and SNRs. Preliminary experiments with SSFP fluoroscopy in human volunteers revealed that images of adequate quality can be obtained in 225 milliseconds (Fig 1). The results of these preliminary experiments indicate that temporal resolution is not currently a limiting factor in SSFP MR fluoroscopy.

The clinical use of MR fluoroscopy awaits substantial improvements. Rather than manually prescribing an imaging plane to include the device, the position of the device can be used to automatically define the imaging plane (15, 16). This requires the use of active device guidance. With active guidance, a device-mounted coil receives signals from the adjacent tissue. This signal is used to localize the device. Replacing the current method for defining the imaging plane will allow for simplified navigation, and the operator can focus on manipulating the device. Active tracking with automatic definition of the imaging plane would also ensure that a predetermined point or segment of the microcatheter-microguidewire lies within the imaging plane. This ability would not only aid navigation but also improve safety.

Conclusion

SSFP MR fluoroscopy provides adequate contrast and temporal resolution, and the images are resistant to artifacts. SSFP image quality was sufficient to allow for microcatheter and microguidewire manipulation in the intracranial subarachnoid space by using the passive tracking technique. Substantial improvements are underway to extend the clinical utility of MR imaging–guided intracranial navigation with PIN.

References

1. Purdy PD, Replogle RE, Pride GL, Adams C, Miller S, Samson D. **Percutaneous intraspinal navigation (PIN): a feasibility study in cadavers of a new and minimally invasive approach to the spinal cord and brain.** *Am J Neuroradiol*. In press.
2. Hamada J, Mizuno T, Kai Y, Morioka M, Ushio Y. **Microcatheter intrathecal urokinase infusion into cisterna magna for prevention of cerebral vasospasm: preliminary report.** *Stroke* 2000;31:2141–2148
3. Mueller PR, Stark DD, Simeone JF, et al. **MR-guided aspiration biopsy: needle design and clinical trials.** *Radiology* 1986;161:605–609
4. Mahfouz AE, Rahmouni A, Zylbersztejn C, Mathieu D. **MR-guided biopsy using ultrafast T1- and T2- weighted reordered turbo fast low-angle shot sequences: feasibility and preliminary clinical applications.** *AJR Am J Roentgenol* 1996;167:167–169
5. Lewin JS, Connell CF, Duerk JL, et al. **Interactive MRI-guided radiofrequency interstitial thermal ablation of abdominal tumors: clinical trial for evaluation of safety and feasibility.** *J Magn Reson Imaging* 1998;8:40–47
6. Wacker FK, Reither K, Branding G, Wendt M, Wolf KJ. **Magnetic resonance-guided vascular catheterization: feasibility using a passive tracking technique at 0.2 Tesla in a pig model.** *J Magn Reson Imaging* 1999;10:841–844
7. Spuentrup E, Ruebben A, Schaeffter T, Manning WJ, Gunther RW, Buecker A. **Magnetic resonance–guided coronary artery stent placement in a swine model.** *Circulation* 2002;105:874–879
8. Oppelt A, Graumann R, Barfu H, Fisher H, Hartl W, Schajor W. **Fisp-a new fast MRI sequence.** *Electromedica* 1986;54:15–18
9. Haacke EM, Tkach JA. **Fast MR imaging techniques and clinical applications.** *AJR Am J Roentgenol* 1990;5:951–964
10. Duerk JL, Lewin JS, Wendt M, Petersilge C. **Remember true FISP? A high SNR, near 1-second imaging method for T2- like contrast in interventional MRI at .2 T.** *J Magn Reson Imaging* 1998;8:203–208
11. Chung YC, Merkle EM, Lewin JS, Shonk JR, Duerk JL. **Fast T(2)-weighted imaging by PSIF at 0.2 T for interventional MRI.** *Magn Reson Med* 1999;42:335–344
12. Haacke EM, Wielopolski PA, Tkach JA, Modic MT. **Steady-state free precession imaging in the presence of motion: application for improved visualization of the cerebrospinal fluid.** *Radiology* 1990;175:545–552
13. Chung HW, Chen CY, Zimmerman RA, Lee KW, Lee CC, Chin SC. **T2-weighted fast MR imaging with true FISP versus HASTE: comparative efficacy in the evaluation of normal fetal brain maturation.** *AJR Am J Roentgenol* 2000;175:1375–1380
14. Plein S, Bloomer TN, Ridgway JP, Jones TR, Bainbridge GJ, Sivananthan MU. **Steady-state free precession magnetic resonance imaging of the heart: comparison with segmented k-space gradient-echo imaging.** *J Magn Reson Imaging* 2001;14:230–236
15. Zhang Q, Wendt M, Aschoff AJ, Zheng L, Lewin JS, Duerk JL. **Active MR guidance of interventional devices with target-navigation.** *Magn Reson Med* 2000;44:56–65
16. Buecker A, Adam GB, Neuerberg JM, et al. **Simultaneous real-time visualization of the catheter tip and vascular anatomy for MR guided PTA of iliac arteries in an animal model.** *J Magn Reson Imaging* 2002;16:201–208